



HAL
open science

Towards Self-Adaptive Parameterization of Bézier Curves for Airfoil Aerodynamic Design

Zhi Li Tang, Jean-Antoine Desideri

► **To cite this version:**

Zhi Li Tang, Jean-Antoine Desideri. Towards Self-Adaptive Parameterization of Bézier Curves for Airfoil Aerodynamic Design. [Research Report] RR-4572, INRIA. 2002. inria-00072016

HAL Id: inria-00072016

<https://inria.hal.science/inria-00072016>

Submitted on 23 May 2006

HAL is a multi-disciplinary open access archive for the deposit and dissemination of scientific research documents, whether they are published or not. The documents may come from teaching and research institutions in France or abroad, or from public or private research centers.

L'archive ouverte pluridisciplinaire **HAL**, est destinée au dépôt et à la diffusion de documents scientifiques de niveau recherche, publiés ou non, émanant des établissements d'enseignement et de recherche français ou étrangers, des laboratoires publics ou privés.

Towards Self-Adaptive Parameterization of Bézier Curves for Airfoil Aerodynamic Design

Zhi Li Tang – Jean-Antoine Désidéri

N° 4572

September 2002

THÈME 4



*R*apport
de recherche

Towards Self-Adaptive Parameterization of Bézier Curves for Airfoil Aerodynamic Design

Zhi Li Tang * – Jean-Antoine Désidéri †

Thème 4 — Simulation et optimisation
de systèmes complexes
Projet Opale

Rapport de recherche n° 4572 — September 2002 — 20 pages

Abstract: This report is part of a series of numerical studies in optimum-shape design in aerodynamics in which the equations of Fluid Mechanics (typically the Euler Equations for Compressible Perfect Gas) are solved by a Finite-Volume-type method over a structured or unstructured mesh, and the aerodynamic shape (wing or airfoil) is optimized w.r.t. some aerodynamic criterion (e.g. lift maximization or drag reduction). We are considering here the two-dimensional case in which the shape is an airfoil represented by a Bézier curve whose degree is much smaller than the number of meshpoints on the body surface and we assume that the control points have *a priori* fixed abscissas and that their ordinates constitute the set of parameters of the optimization. We evaluate by numerical experiments the incidence of this *a priori* choice on the efficacy of the optimization.

Key-words: Bézier curve, airfoil, aerodynamics, optimum shape design

Projet OPALE : Optimisation et contrôle, algorithmes numériques et intégration de systèmes complexes multidisciplinaires régis par des E.d.p. (<http://www.inria.fr/recherche/equipes/opale.fr.html>)

OPALE Project : Optimization and Control, Numerical Algorithms and Integration of Complex Multi-Disciplinary Systems governed by P.D.E. (<http://www.inria.fr/recherche/equipes/opale.en.html>)

* P.O. Box 1006, 29, YuDao St., Nanjing University of Aeronautics and Astronautics, Nanjing, 210016, P.R. China, tangzhili@hotmail.com

† Jean-Antoine.Desideri@sophia.inria.fr

Vers une paramétrisation automatique de courbes de Bézier pour l'optimisation aérodynamique de profils

Résumé : Ce rapport s'insère dans le cadre d'études numériques en conception optimale de forme aérodynamique dans lesquelles les équations de la Mécanique des Fluides (typiquement les équations d'Euler pour un fluide parfait compressible) sont résolues par une méthode de type Volumes-Finis sur un maillage structuré ou non, et la forme aérodynamique (aile ou profil) est optimisée vis-à-vis d'un critère aérodynamique (e.g. maximisation de portance ou réduction de traînée). On se place ici dans le cas bidimensionnel où la forme est un profil d'aile représenté par une courbe de Bézier dont le degré est très inférieur au nombre de points de maillage sur le contour et on suppose que les points de contrôle ont des abscisses fixées *a priori* et que leurs ordonnées constituent les paramètres de l'optimisation. On évalue par une série d'expériences numériques l'incidence de ce choix *a priori* sur l'efficacité de l'optimisation.

Mots-clés : Courbe de Bézier, profil d'aile, aérodynamique, conception optimale de forme

1 Introduction

Over the past twenty years, scientific computing has achieved considerable potential for solving Partial Differential Equations (PDEs), permitting the scientist and the engineer to simulate numerically a large variety of nonlinear phenomena accurately. The merit for such achievement owes fairly evenly to the progress of Numerical Analysis (and High-Performance Computing) as to the enhanced computing resource. In particular, *compressible-flow solvers* are used on a daily basis in Industry not only in predictive computations, but also in the design loop, introducing today, even more complex multi-disciplinary concepts.

The present study fits in this current trend in which numerical approaches are devised for optimum-shape design in Aerodynamics as in [1] and related multi-disciplinary applications. One of our main current concerns resides in the adaptation of the geometrical parameterization [2] [3] [4] [5] [6] since in practical applications, the number of boundary meshpoints far exceeds the number of design parameters standard optimizers can usually handle.

For the purpose of introduction, let us consider the demonstrative fundamental example problem of optimum airfoil shape design for pressure-drag reduction in Eulerian flow. Clearly this model will need to be ultimately refined for realistic applications. One has to minimize a functional of the airfoil shape represented here by two functions $y^\pm(x)$ (upper and lower surfaces) subject to several constraints, including : $y^\pm(0) = 0$, $y^\pm(1) = 0$, $dy^\pm/dx(0) = \pm\infty$, $0 \leq y^+(x) - y^-(x) \leq \delta$, etc :

$$C_D = C_D[y] = \int_{\gamma} p dy = \int_0^1 \pm p^\pm(x) \frac{dy^\pm}{dx}(x) dx \quad (1)$$

Technically, the shape is represented by a finite set of parameters, some of which are chosen *a priori*, the remaining being subject to the optimization process (via a flow solver). For example, an airfoil can be smoothly represented by a Bezier curve [7], formally parameterized by Bernstein polynomials :

$$\begin{cases} x_B(t) = \sum_{k=0}^n x_k B_n^k(t) \\ y_B(t) = \sum_{k=0}^n y_k B_n^k(t) \end{cases} \quad (2)$$

where $t \in [0, 1]$ is a parameter varying continuously, $B_n^k(t) = C_n^k t^k (1-t)^{n-k}$ ($k = 0, 1, \dots, n$) is a Bernstein polynomial of degree n , and, at this stage, (x_k, y_k) are coefficients. In these formulas, $x_B(t)$ and $y_B(t)$ are polynomials of degree n (at most) of the parameter t , and from a pure algebraic point of view, the introduction of the Bernstein basis neither enhances nor restricts this general statement. The advantage of this particular expression relies mostly in the algorithmic point of view, since the coefficients (x_k, y_k) can be viewed as the coordinates of control points that can be placed with some intuition according to the expected shape main characteristics : thus, generally, one selects a 'reasonable' set of abscissas, $\{x_k\}$, maintained fixed while optimizing the ordinates $\{y_k\}$, reducing in this way the total number of design parameters to $n - 1$ (assuming given endpoints). Therefore intuition provides the practitioner with some guidance. Additionally, a number of geometrical constraints can easily be enforced in such representation, in particular slopes, and more generally finite Taylor's series expansions, at endpoints. However, Approximation Theory (applied to functions and curves) teaches us that if such an approach is used, the quality of the curvefit, and thus, the aerodynamic design, is strongly conditioned by the *a priori* choice made for the abscissas.

Our driving objective is to devise adaptive algorithms to revise this *a priori* choice in a sensible way, possibly using a partial knowledge of the solution.

One possibility for achieving this could be to render the numerical approximation of the above functional as close as possible to a Gaussian quadrature, which, in a sense, is exact over a 'maximal set' of polynomials. To state this classical result more precisely, consider the case of the numerical approximation of the following integral :

$$I[f] = \int_a^b f(x) dx = \int_a^b g(x) w(x) dx \quad (3)$$

in which the original integrand $f(x)$ has been purposely formatted as the product of two factors with complementary characteristics :

- $g(x)$, a function that has the merit of being smooth, but nonlinear in a way that permits no formal calculation (no primitive function known),
- $w(x)$ a weighting function, that contains the possible singularities of the original integrand at endpoints, but such that the integrals $\int_a^b x^\alpha w(x) dx$ (for all integers $\alpha \leq n$) are known exactly (or computed accurately once for all or adaptively).

The standard numerical technique, in short, consists in first approximating the smooth function $g(x)$ by an interpolation polynomial $P_n(x)$, and second, in approximating the value of the functional $I[f]$ by substituting in it $P_n(x)$ in place of $g(x)$ and carrying out the remaining calculations exactly, which is possible by hypothesis on w .

On one hand, the interpolation error has the form :

$$e_n(x) = g(x) - P_n(x) = (x - x_0)(x - x_1)\dots(x - x_n) \frac{g^{(n+1)}(\xi)}{(n+1)!} \quad (4)$$

This formula, from which the standard Lagrange remainder in the finite Taylor's expansion of $g(x)$ can be derived, involves the intermediate value of the $n + 1$ st derivative of g at some unknown point ξ ; as a result, unsurprisingly, the interpolation is uniformly exact iff $g(x)$ is a polynomial of degree n at most.

However, the integration error,

$$E = I[f] - I[P_n w] = \int_a^b e_n(x) w(x) dx \quad (5)$$

can usually be given the form :

$$E = C (b - a)^{\nu+1} g^{(\nu)}(\eta) \quad (6)$$

where C is a numerical constant, $\eta \in [a, b]$ another unknown intermediate point, and the order of the derivative ν is a preferably large integer. While for any choice of the $n + 1$ interpolation points, $\{x_k\}$ ($0 \leq k \leq n$), the form of the interpolation error implies that $\nu \geq n + 1$, the particular choice corresponding to the Gaussian rule, based on the zeros of the orthogonal polynomials that are associated with the inner product :

$$(u, v) = \int_a^b u(x) v(x) w(x) dx \quad (7)$$

(note the importance of the chosen weighting function $w(x)$), permits to achieve $\nu = 2n + 2$, and this is maximal, thus making the numerical integration exact over the set of polynomials of degree $2n + 1$ (at most), that is, over a class of polynomials roughly speaking twice as large in dimension. The increase in accuracy is usually spectacular.

An alternate interpretation of this result is to say that the Gaussian points are the points which mostly affect the numerical evaluation of the integral, and in this respect, it becomes intuitive that they should be chosen as natural support to optimize the shape, via aerodynamics or other possibly coupled disciplines. Therefore, the question is for a given discipline, what is the right split between smooth and weighting factors g and w of the integrand. This identification will be used to guide the choice of the abscissas supporting the parameterization.

With these concepts in mind, we experiment in this report a number of alternative Bézier parameterizations to either approximate a given curve or evaluate the efficacy of an airfoil drag reduction.

2 A series of numerical experiments to evaluate and adapt the parameterization

2.1 Bézier curvefit of a function given analytically

In the first experiment, we consider the problem of approximating a given target curve, defined analytically by the function

$$y_T(x) = cx^a(1-x)^b + dx(1-x) \quad x \in [0, 1] \quad (8)$$

(typically : $a = 0.5$, $c = 0.15$, $b = 1.0$, $d = 0.01$).

A discrete analog of the L2-norm of the difference between the above function $y_T(x)$ and the function $y_B[t(x)]$ defined implicitly by (2) is given by :

$$j = \sqrt{\sum_{i=1}^{N_P} |y_B(t_i) - y_T[x_B(t_i)]|^2 \delta x_i} \quad (9)$$

where :

$$\delta x_i = \frac{x_B(t_{i+1}) - x_B(t_{i-1})}{2} \quad (10)$$

and $i = 1, 2, \dots, N_P$, $t_i = (i-1)/(N_P-1)$, $N_P \gg n$ ($N_P = 130$).

For a fixed degree n , j is a function of the coordinates (x_k, y_k) ($k = 0, 1, \dots, n$) of the control points defining the Bézier curve.

We have used the routine E04JYF from the NAG library to minimize j in three different cases:

1. Uniform distribution (of abscissas $\{x_k\}$) :
 $x_k = k/n$, $y_0 = y_n = 0$; y_1, y_2, \dots, y_{n-1} : free
2. Cosine distribution :
 $x_k = \{1 + \cos[(2k+1)\pi/(2n+2)]\}/2$; $y_0 = y_n = 0$, y_1, y_2, \dots, y_{n-1} : free
3. Fully optimized parameters :
 $x_0 = x_1 = 0$, $x_n = 1$, $y_0 = y_n = 0$; x_2, x_3, \dots, x_{n-1} and y_1, y_2, \dots, y_{n-1} : free

The ‘‘cosine’’ distribution is inspired from the concept of ‘‘best interpolation polynomial’’ and Chebychev economization [8].

In the third case, the constraints enforce that the endpoints of the Bézier curve actually be (0,0) and (0,1), and that the tangent at the origin be vertical.

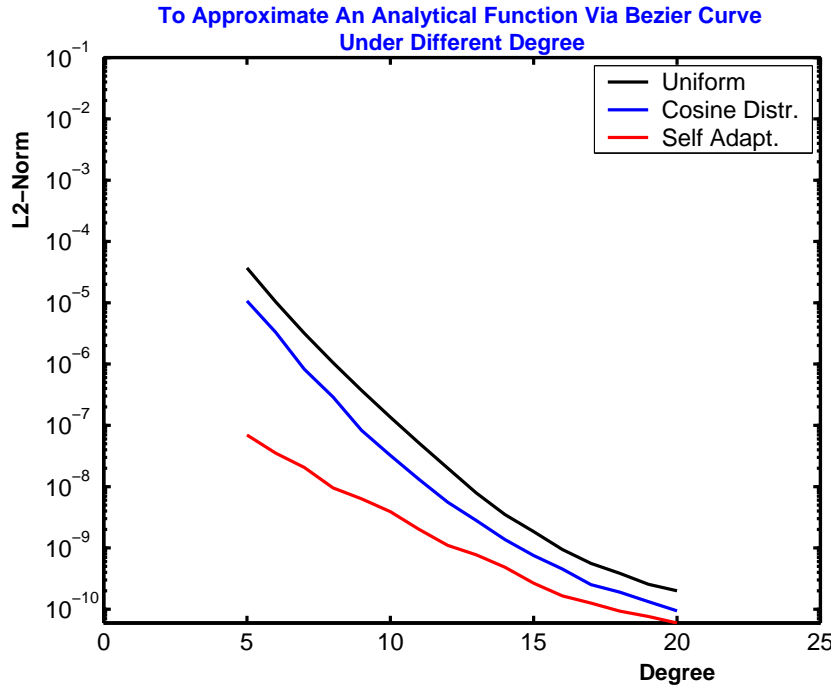


Figure 1: Bézier curvefit of a function defined analytically

The results of the minimization for varying n is indicated on Figure 1, in which the colors black, blue and red correspond to cases 1, 2 and 3 respectively.

It appears that the cosine distribution, often used in practice, indeed gives somewhat more accurate results than a uniform distribution, but the difference is not very large. However, when optimizing numerically the abscissas as well as the ordinates, the improvement is very significant, particularly for a small degree n . In practice, we often use $n = 8$. Asymptotically, however they seem equivalent.

2.2 Bézier curvefit of the RAE2822 airfoil

A similar experiment has been conducted in the case where the target curve, instead of being defined analytically, is a known airfoil, the RAE2822 airfoil, defined by a discrete set of values (x_{T_i}, y_{T_i}) , $i = 1, 2, \dots, N_T$ ($N_T = 47$).

The corresponding results of optimization are given on Figure (2) with the same color correspondance. Again, unsurprisingly, the optimization of the whole set of coordinates outperforms the other two methods, but the difference is less significant. This is likely due to the fact that the interpolation of the target curve at the points $\{t_i\}$ was carried with insufficient accuracy (second-order). Thus we observe the rapid loss of accuracy due to the transfer of data from one format to another. This question, formulated in a more general context, would deserve a more thorough examination, particularly in a framework where data are often transferred or exchanged from one grid to another.

2.3 Inverse aerodynamic design

Here, instead of approximating a geometrical target curve, the parameters (y_k 's or (x_k, y_k) 's) are optimized according to the previous three rules (1. uniform distribution of abscissas, 2. cosine

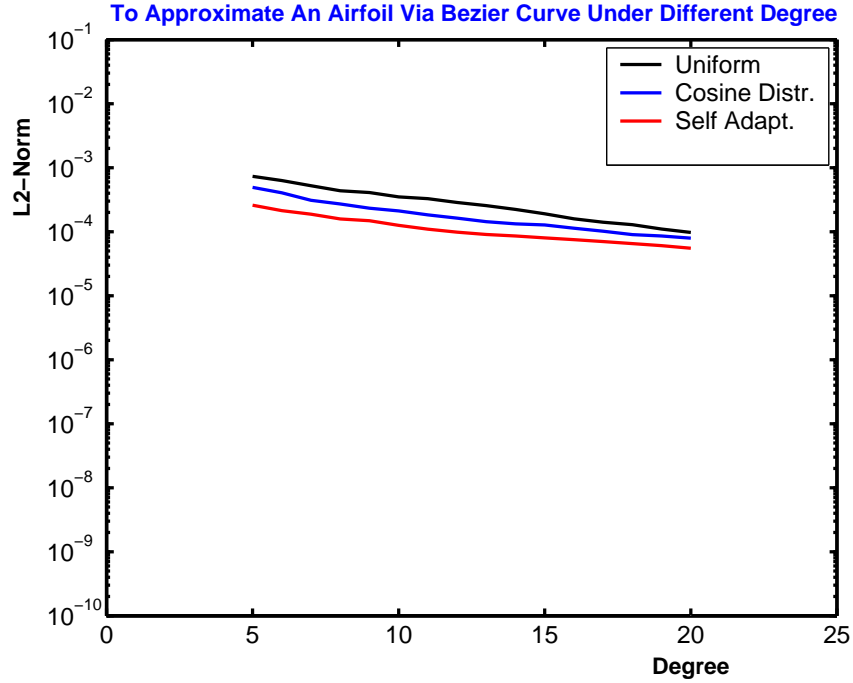


Figure 2: Bézier curvefit of the RAE2822 airfoil

distribution, 3. full optimization) to minimize the discrepancy between the calculated body-surface pressure p and a target pressure distribution p_d measured by the functional :

$$I = \frac{1}{2} \oint_c (p - p_d)^2 ds \quad (11)$$

The design case corresponds to the conditions : $M_\infty = 0.73$, $\alpha = 2.0^\circ$; p_d is the pressure distribution over the RAE2822 airfoil in these conditions. The corresponding iso-Mach number contours are depicted on Figure 3, over which the shock wave over the upper surface is clearly visible and its reduction is the focus of the optimization in subsequent experiments.

Note that this target airfoil is not a Bézier curve, thus $I \neq 0$ at convergence of the inverse problem.

The minimum value of I is given on Figure 4 for various degree n for the three types of distribution of control points.

Here the cosine distribution and the fully-optimized distribution of control points perform very significantly better than the method based on a uniform distribution, corresponding to a reduction of the functional of about two orders of magnitude more at convergence. For a low degree, the cosine distribution is almost as performant as the fully optimized, but the trend is not constant, making this “rule-of-thumb” hazardous.

Hence, optimizing the parameterization has the potential to significantly enhance the quality of the physical solution.

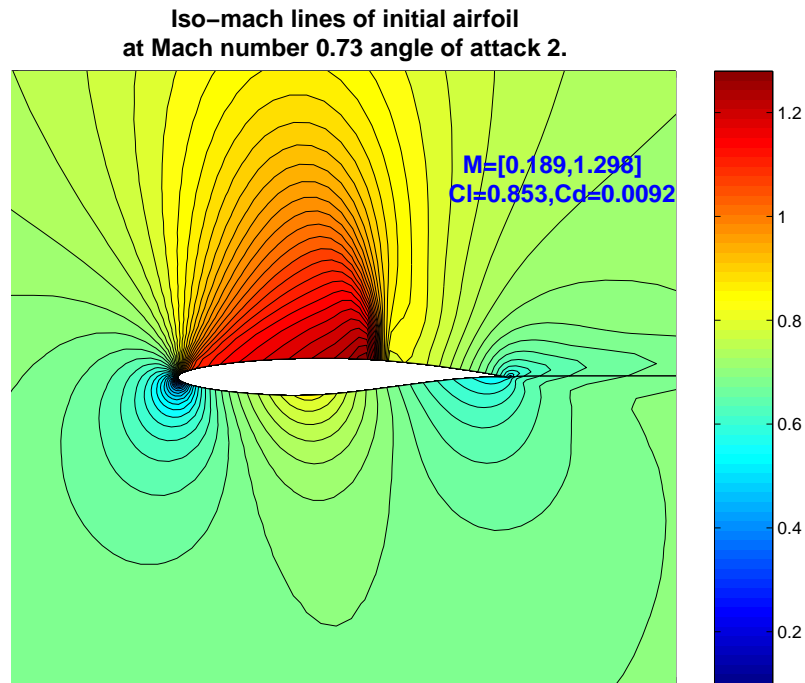


Figure 3: Iso-Mach number contours around RAE2822 airfoil ($M_\infty = 0.73$, $\alpha = 2^\circ$)

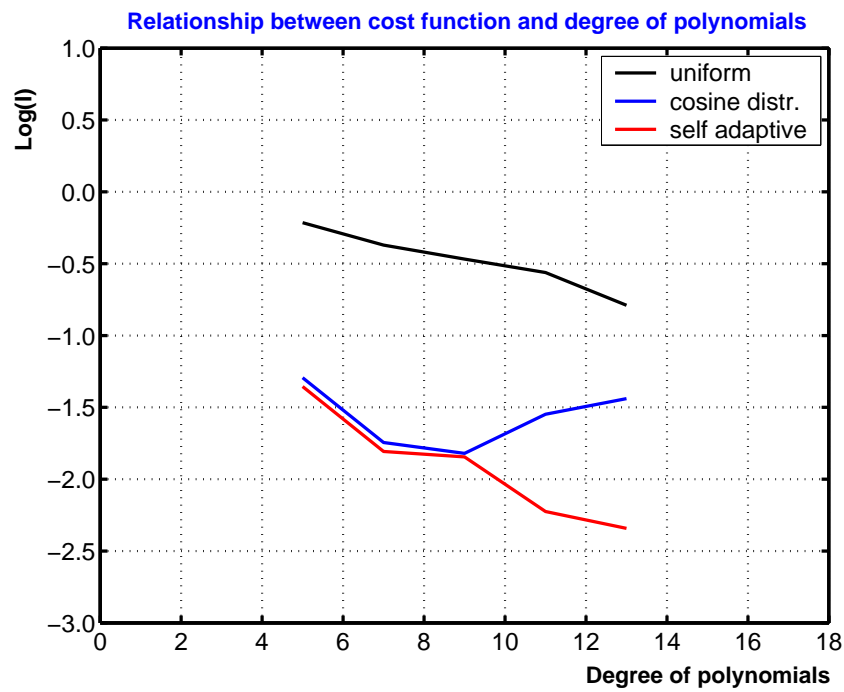


Figure 4: Quality of inverse aerodynamic design depending on the *a priori*-defined Bézier parameterization

2.4 Non-unicity of best Bézier curvefit

We have repeated the experiment of subsection 2.1 in which a function defined analytically and whose curve is not a Bézier curve, is best fitted by a Bézier curve of degree 8.

The results are indicated on Figure 5. They indicate that for two different initial conditions, the optimization routine achieves two very different sets of optimized parameters, both yielding a very good approximation of the same curve. This is not surprising since the Bézier representation is not unique [7].

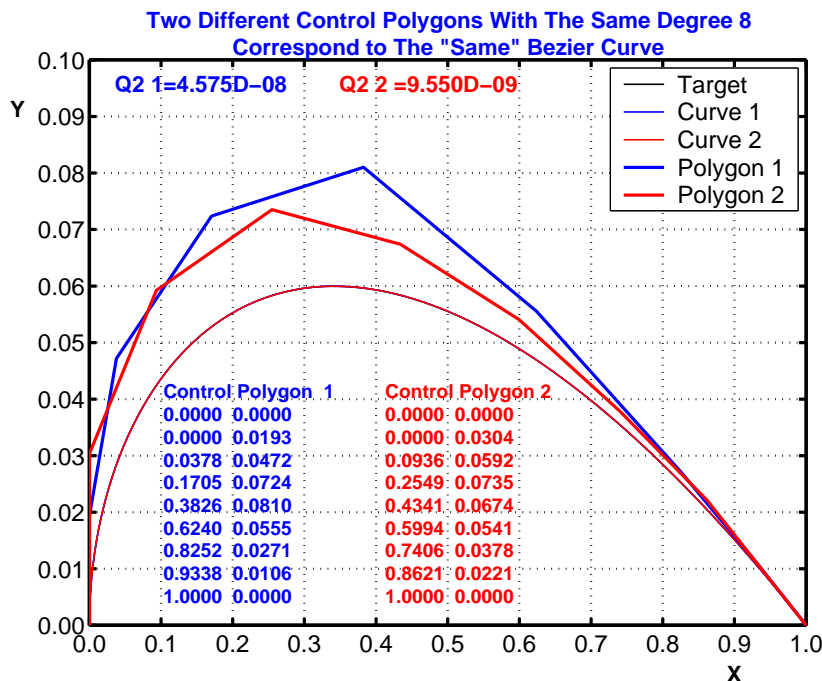


Figure 5: Non-unicity of best Bézier curvefit

2.5 Bézier curvefit with a regularity constraint based on the total variation

We are aiming at devising a self-adaptive parameterization to be coupled with an optimization loop. Basically, we propose that while the y_k 's are classically optimized w.r.t. some physical criterion (for fixed x_k 's), to alternatively optimize the x_k 's w.r.t. a geometrical regularity criterion.

As a step towards this, we again consider the problem of curvefitting a target curve (to be replaced subsequently by the freshest update of the optimized shape) by relocating the abscissas of the control points to minimize a regularity violation measure, such that the total-variation in the ordinates of the control points :

$$TV(\{y_k\}) = \sum_{i=1}^n |y_k - y_{k-1}| \tag{12}$$

Consequently, given a target curve, the abscissas $\{x_k\}$ are redefined to solve the following constrained minimization problem :

$$\begin{cases} \min_{\{x_k, y_k\}} TV(\{y_k\}) \\ Q_2 \leq \varepsilon \\ x_0 \leq x_1 \leq x_2 \leq \dots \leq x_n \end{cases} \quad (13)$$

where ε is a sufficiently small positive tolerance ($\varepsilon = 0.0005$ below), and Q_2 is the L_2 -norm between *Bézier* curve and target, calculated discretely. Again, the RAE2822 airfoil is used as a target curve, and the degree $n = 8$.

The result of this curvefit is given on Figure 6 which demonstrates the very good accuracy of the procedure.

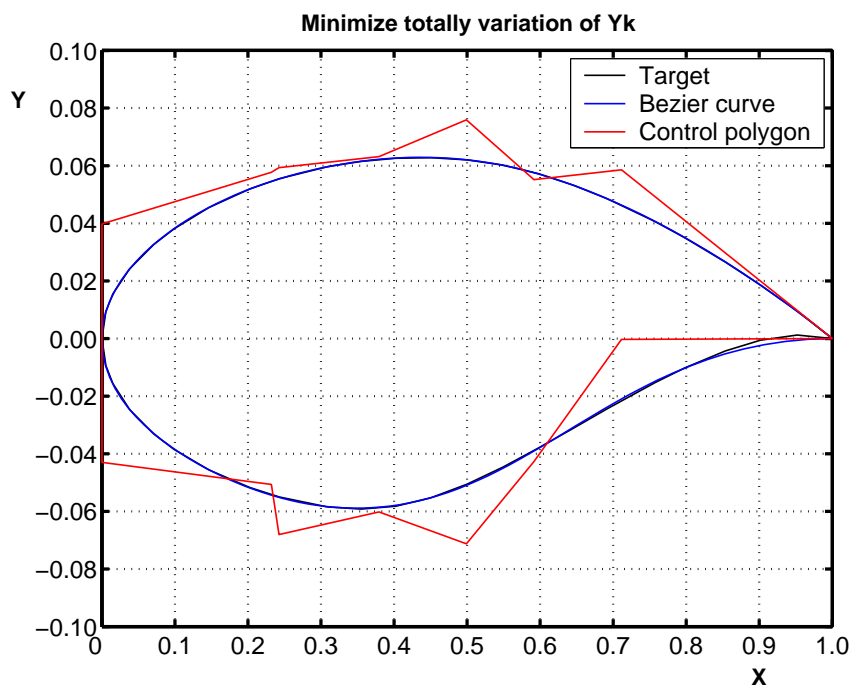


Figure 6: Bézier curvefit with a regularity constraint based on the total variation

2.6 Bézier curvefit with a regularity constraint based on the total length

The experiment is similar to the above, except that in the minimization problem, (13), the total-variation is now replaced by the length of the control polygon (which also represents a regularizing penalty) :

$$L = \sum_{k=1}^n \sqrt{(x_k - x_{k-1})^2 + (y_k - y_{k-1})^2} \quad (14)$$

The corresponding curvefit is indicated on Figure 7. It is again of great quality. We observe in the cases of Figures 6 and 7, that the control polygons are rather close the airfoil curve itself, which is the result of regularization.

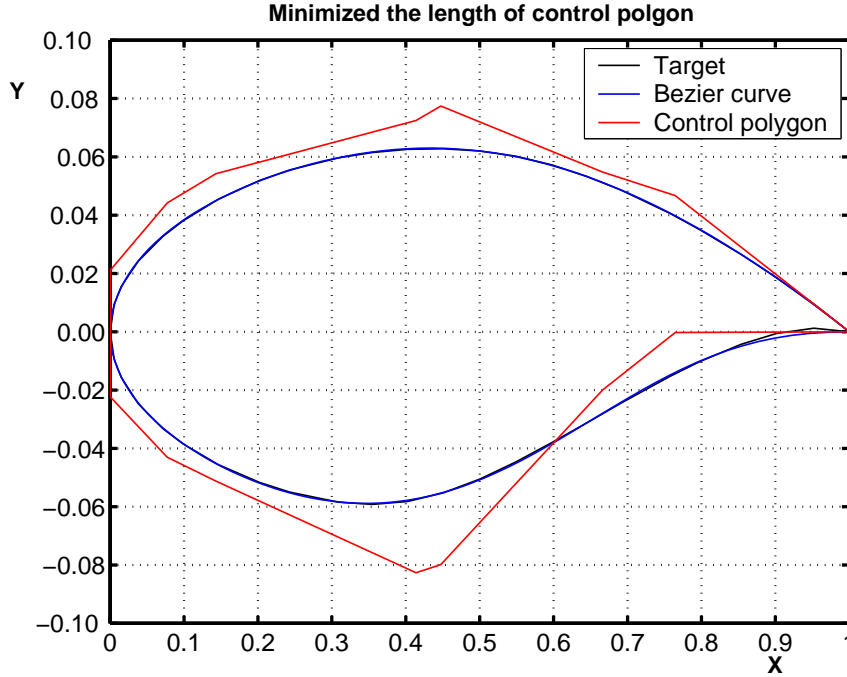


Figure 7: Bézier curvefit with a regularity constraint based on the total length

2.7 Drag reduction based on a uniformly-distributed control points

In this experiment, a pressure-drag reduction is conducted using the RAE2822 airfoil as initial design. The physical conditions of the experiment are : $M_\infty = 0.73$, $\alpha = 2^\circ$. This process is split into two steps. In the first, the RAE airfoil is curvefitted by a Bézier curve using a prescribed set of abscissas for the control points; in the second, using the same fixed abscissas, the drag is reduced by optimizing the ordinates.

The aim of this experiment is to demonstrate that the accuracy of the curvefit alone (which conditions the parameterization employed subsequently) has an important effect on the result of the drag reduction.

Thus, the two steps are defined as follows :

step 1:

$$\begin{cases} \min_{\{y_k\}} j \\ y_0 = y_8 = 0 \end{cases} \quad (15)$$

using the RAE airfoil as a target and a prescribed uniform distribution of x_k 's. Get initial pressure distribution p_i and initial values for the parameters y_k 's.

step 2:

$$\begin{cases} \min_{\{y_k\}} I \\ y_0 = y_8 = 0 \end{cases} \quad (16)$$

where I is the following functional :

$$I = \Omega_1 \frac{1}{2} \oint_c (p - p_i)^2 ds + \Omega_2 C_d \quad (17)$$

(Ω_1 and Ω_2 are two penalty weights; $\Omega_1 = 0.1$, $\Omega_2 = 2.9$ in the experiment). This cost function indicates that the airfoil pressure-drag is to be reduced by a small modification of the initial geometry.

After conducting the two subsequent steps, the drag coefficient C_d is reduced from 0.0097 to 0.0035. The corresponding initial and optimized pressure distributions, and final iso-Mach number contours are given on Figures 8 and 9. The shock strength has visibly been reduced.

2.8 Drag reduction using a parameterization regularized by means of the total variation

This experiment differs from the previous in the way the abscissas of control points are calculated in Step 1. Here, Step 1 is the regularized curfit defined by (13).

As a result, a significantly larger pressure-drag reduction is observed, namely from 0.0097 to 0.00309. Even though the parameterization is adapted statically only once, since Step 2 is an optimization with initial condition close to converged, this experiment reflects in a sense a self-adaptive parameterization and demonstrates its effectiveness. The corresponding initial and optimized pressure distributions, and final iso-Mach number contours are given on Figures 10 and 11.

2.9 Drag reduction using a parameterization regularized by means of the total length

This experiment is similar to the previous, except that the regularization of the parameterization conducted in Step 1 consists in minimizing the length L of the control polygon instead of the total variation of the ordinates.

Here C_d is reduced somewhat less, namely from 0.0097 to 0.00315. The corresponding initial and optimized pressure distributions, and final iso-Mach number contours are given on Figures 12 and 13.

2.10 Drag reduction using a parameterization regularized by optimization of the whole set $\{(x_k, y_k)\}$

This experiment is similar to the previous two, except for Step 1, in which now the best Bézier curvefit of the initial RAE airfoil is obtained by optimizing the whole set of coordinates $\{(x_k, y_k)\}$ subject to the usual constraints ($x_0 = x_1 = x_8 - 1 = y_0 = y_8 = 0$) (to minimize the cost function J).

Therefore, the geometric curvefit of the initial shape realizes the global optimum. However the pressure-drag reduction resulting from Step 2, namely from 0.0097 to 0.00322, is not the most important. There is no contradiction in this, since the initial airfoil does not realize the global optimum w.r.t. the cost function (pressure-drag); hence the parameterization that is best-adapted to it, is not necessarily best-adapted to the optimum. The corresponding initial and optimized pressure distributions, and final iso-Mach number contours are given on Figures 14 and 15.

2.11 Self-adaptive optimization using a weighting function

The next two experiments involve a “self-adaptive parameterization” within the optimization loop. More precisely, the sequence Step 1–Step 2 is repeated iteratively, and Step 1 (minimization of the cost function J) is performed to optimize the location of the abscissas of the control points to best curvefit an airfoil that is the RAE2822 airfoil at the first iteration, and the freshest shape update just provided by Step 2 (minimization of the cost function I) at subsequent iterations. The design case again corresponds to : $M_\infty = 0.73$, $\alpha = 2^\circ$ and the degree $n = 8$.

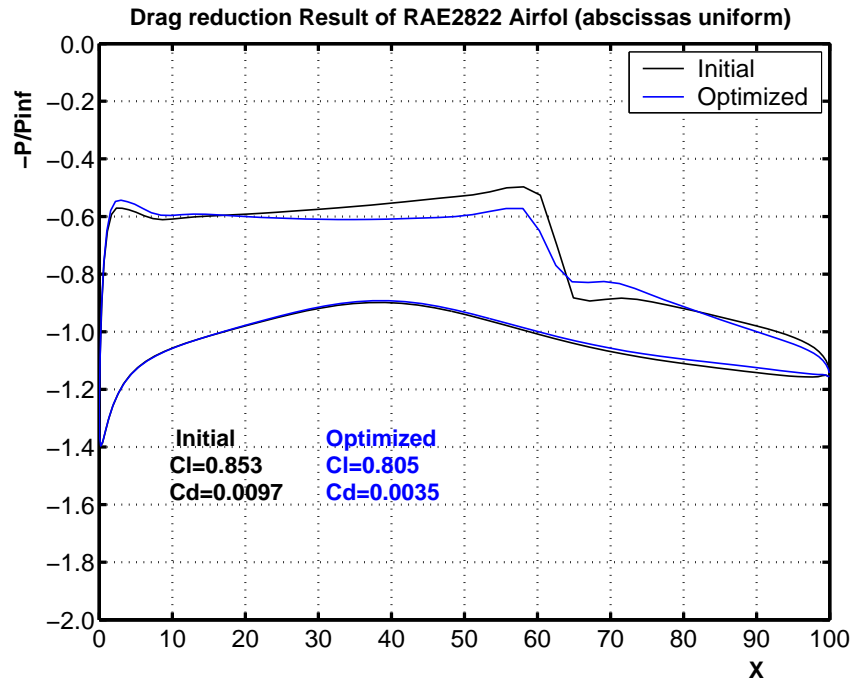


Figure 8: Drag reduction based on uniformly-distributed control points – initial and optimized pressure distribution

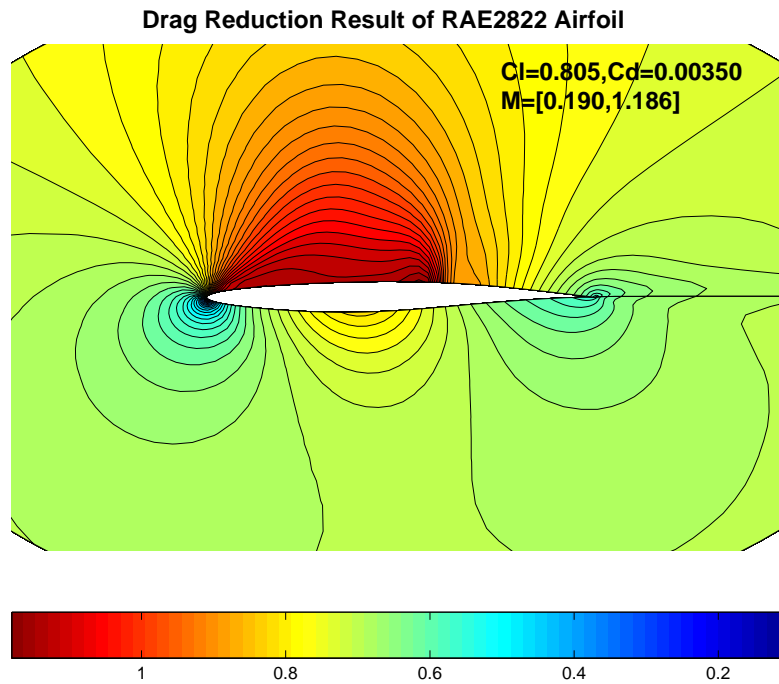


Figure 9: Drag reduction based on uniformly-distributed control points – final iso-Mach number contours

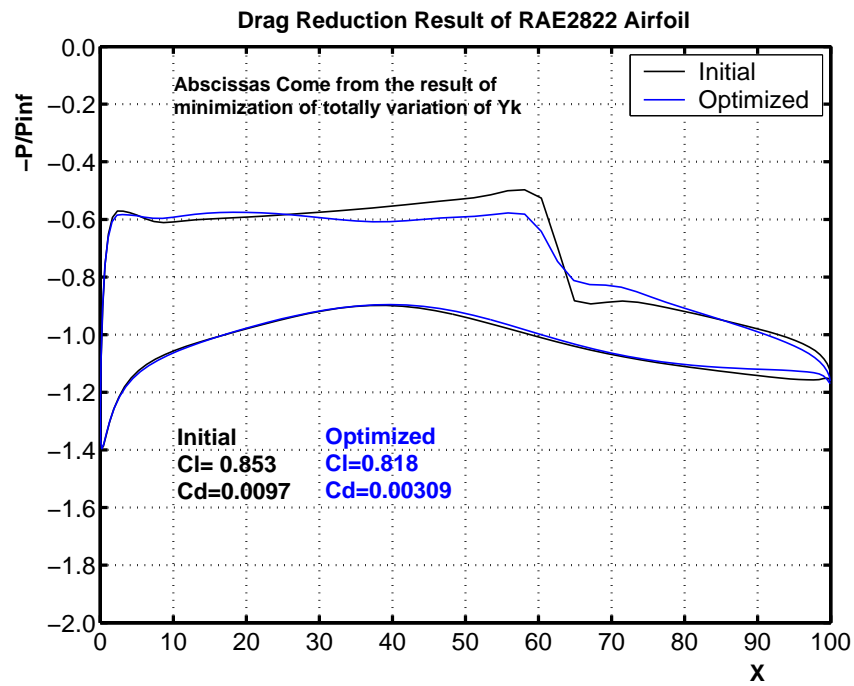


Figure 10: Drag reduction using a parameterization regularized by means of the total variation – initial and optimized pressure distribution

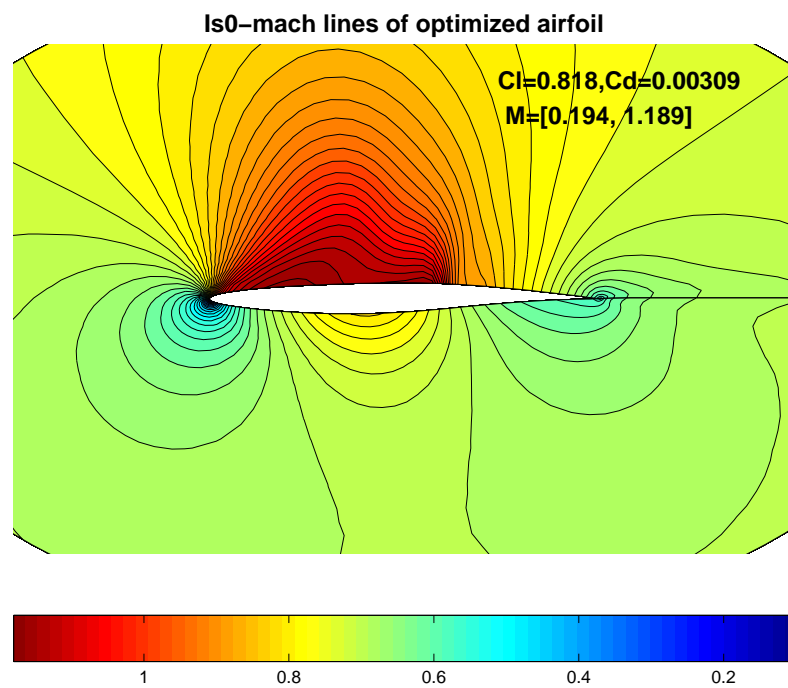


Figure 11: Drag reduction using a parameterization regularized by means of the total variation – final iso-Mach number contours

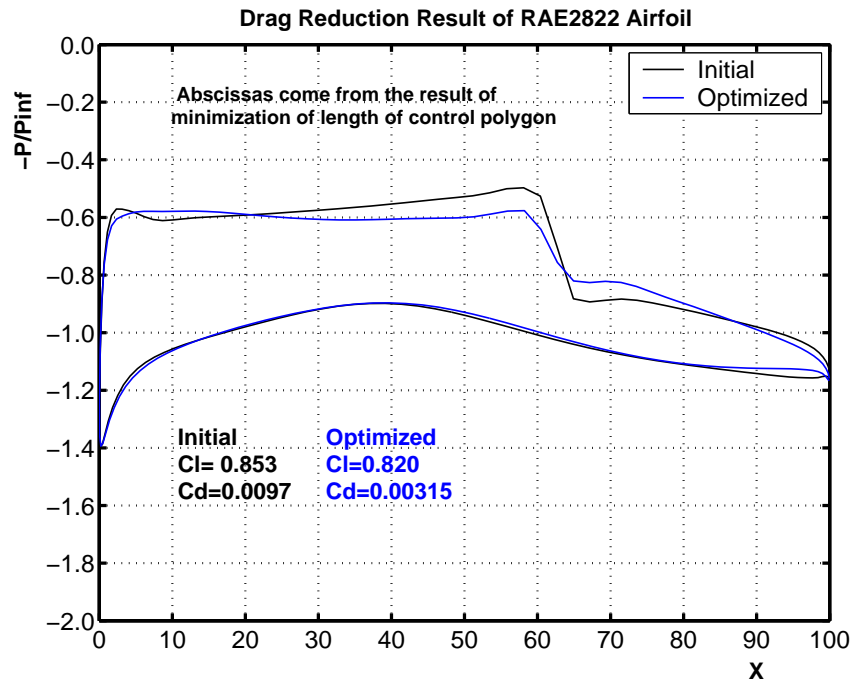


Figure 12: Drag reduction using a parameterization regularized by means of the total length – initial and optimized pressure distribution

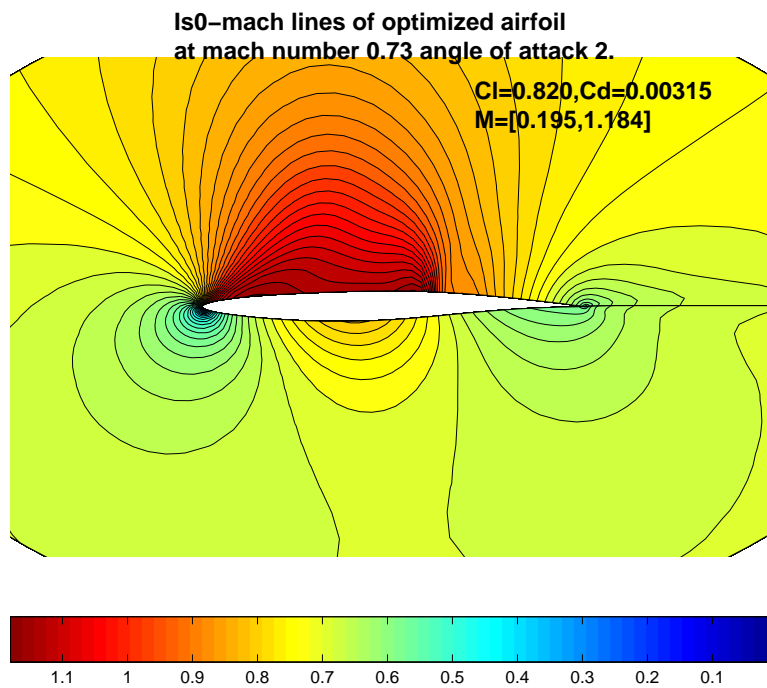


Figure 13: Drag reduction using a parameterization regularized by means of the total length – final iso-Mach number contours

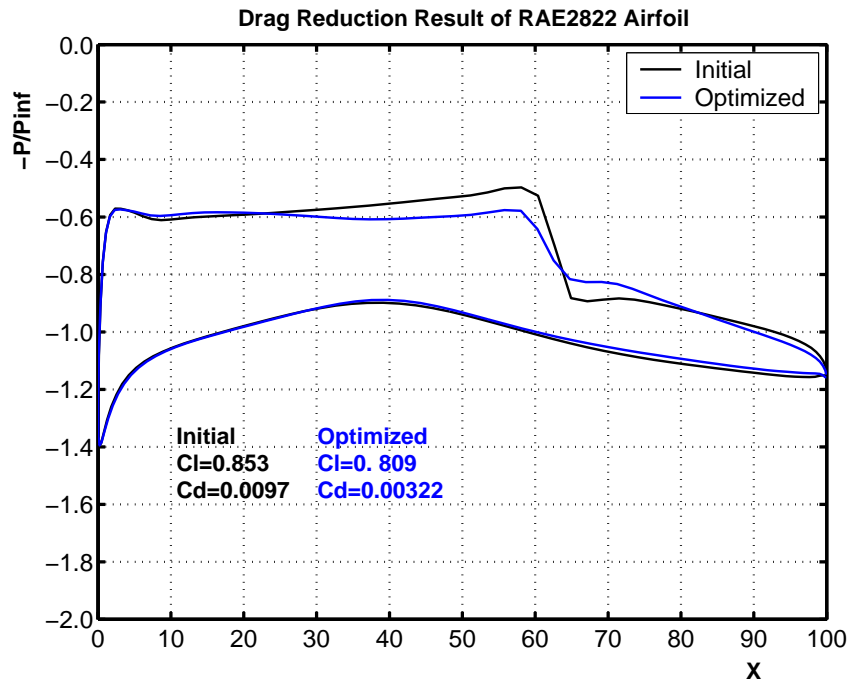


Figure 14: Drag reduction using a parameterization regularized by optimization of the whole set $\{(x_k, y_k)\}$ – initial and optimized pressure distribution

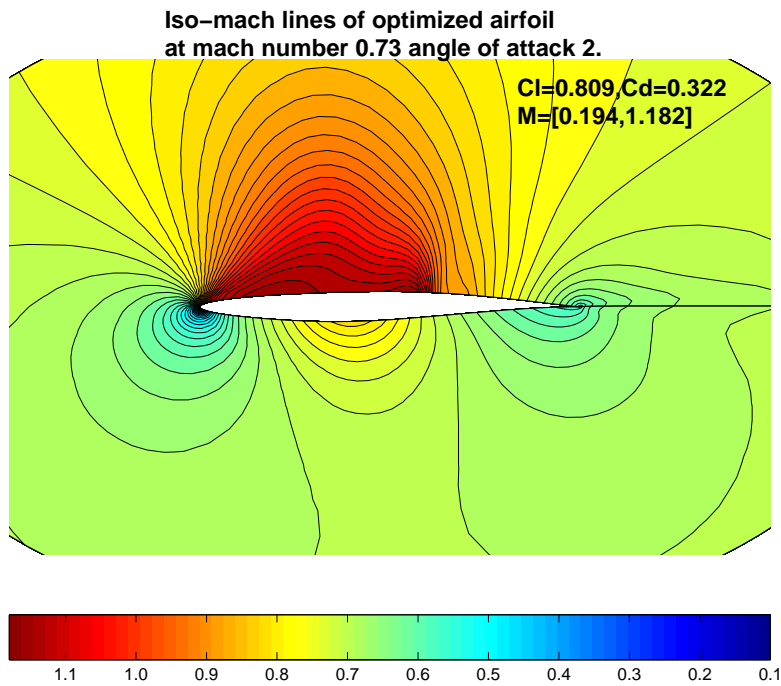


Figure 15: Drag reduction using a parameterization regularized by optimization of the whole set $\{(x_k, y_k)\}$ – final iso-Mach contours

Here, additionally, we are testing the potential of using as control points the zeros of a sequence of orthogonal polynomials $\{P_n(x)\}$ based on a chosen weighting function $w(x)$. These polynomials are generated using a classical algorithm (Algorithm 4.6 of [8]) and the zeros are computed numerically.

Due to the form of the pressure-drag coefficient, it seems interesting to test the following two weighting functions : (i) $w(x) = |y'(x)|$, and (ii) $w(x) = |(p - p_\infty) y'(x)|$.

In case (i), the pressure-drag reduction observed after the first optimization iteration has been from 0.0097 to 0.0049. The corresponding initial and optimized pressure distributions, and final iso-Mach number contours are given on Figures 16 and 17. If the optimization is further continued, after 6 iterations, coefficient is reduced to 0.004131.

In case (ii), after 4 iterations of the process, the pressure-drag coefficient is reduced from 0.0097 to 0.00504, indicating a somewhat less efficient algorithm.

The apparent convergence of this coupled parameterization-adaption/drag-reduction is very encouraging. However, the tested weighting functions are evidently not the most appropriate. More sensible options remain to be identified.

3 Conclusions

In this report, we have conducted a number of numerical experiments in which different Bézier parameterizations of an airfoil have been constructed and compared, in the context of curvefitting first, and then as part of an adaption step within an aerodynamic optimization.

Although further theoretical analysis or more thorough numerical experiments would be useful, our experiments permit us to conclude that :

1. the quality of a Bézier curvefit of given degree depends importantly on the way the abscissas of the control points are prescribed;
2. the Bézier curvefit improves by a regularization technique, such as the minimization of the total variation of the ordinates of the control points;
3. coupling the parameterization regularization with the flow optimization revealed convergent and advantageous.

These guidelines have been used successfully in a (3D) wing optimization [2] for which the geometrical adaption revealed quite effective to achieve larger pressure-drag reductions due to the enhanced search space.

Finally, an interesting open topic will be to examine further techniques inspired from Gaussian quadrature with more sensible splittings of the integrand.

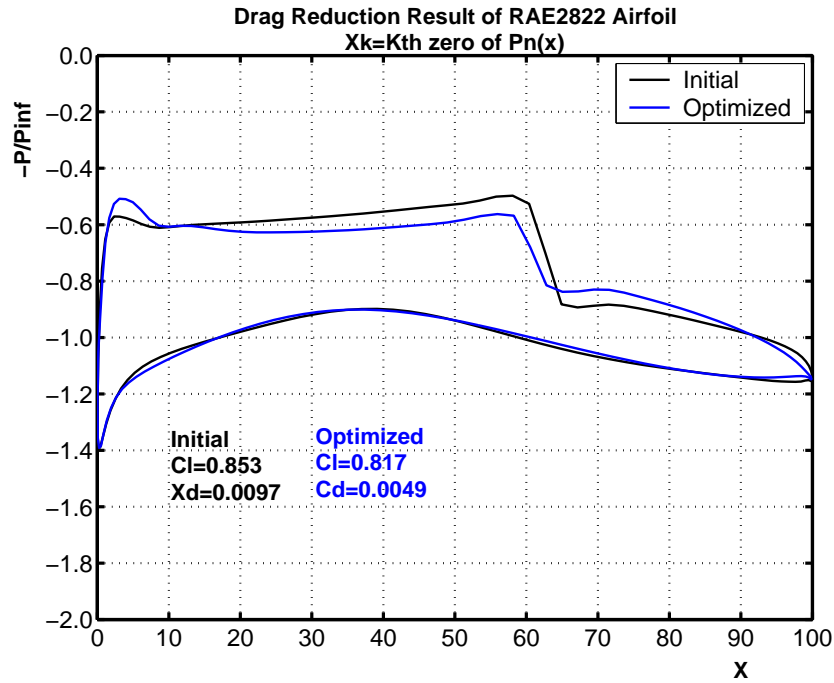


Figure 16: Self-adaptive optimization using a weighting function – initial and optimized pressure distribution

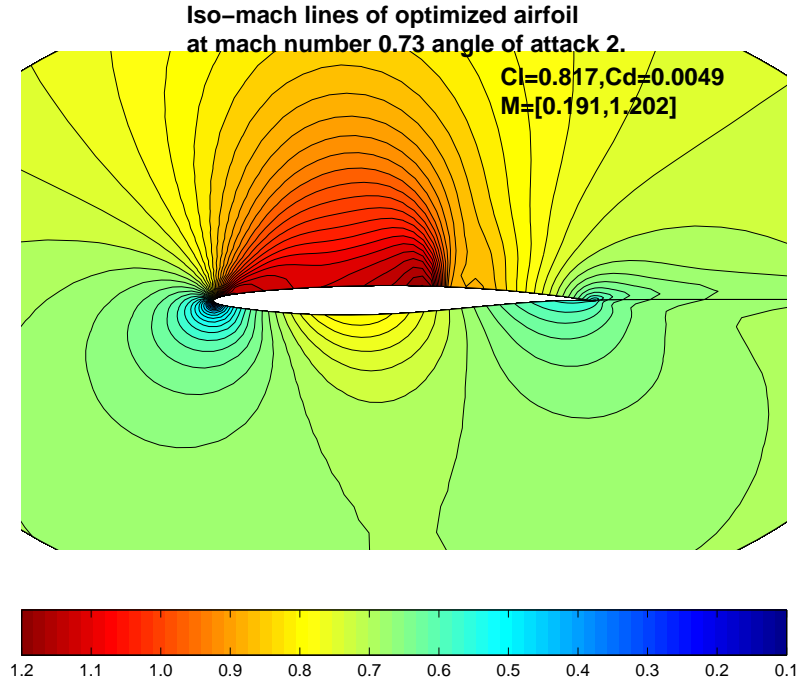


Figure 17: Self-adaptive optimization using a weighting function – final iso-Mach number contours

References

- [1] N. Marco, S. Lantéri, J.-A. Désidéri, B. Mantel, and J. Périaux. Parallelized genetic algorithm for a two-dimensional-shape optimum design problem. *Surveys on Mathematics for Industry*, 9:207–221, 2000.
- [2] A. Clarich and J.-A. Désidéri. Self-adaptive parameterisation for aerodynamic optimum-shape design. Rapport de Recherche 4428, INRIA, March 2002.
- [3] M. Karakasis and J.-A. Désidéri. Model reduction and adaption of optimum-shape design in aerodynamics by neural networks. Rapport de Recherche 4503, INRIA, July 2002.
- [4] Z. Tang, J.-A. Désidéri, and J. Périaux. Distributed optimization using virtual and real game strategies for aerodynamic design. Rapport de Recherche 4543, INRIA, September 2002.
- [5] Z. Tang, J.-A. Désidéri, and J. Périaux. Distributed optimization using virtual and real game strategies for aerodynamic multi-objective design. In D.E. Zeitoun et al., editor, *West East High Speed Flow Fields 2002*, Marseille, France, 2002. CIMNE, Barcelona, Spain. to appear.
- [6] J. Morice, J.-A. Désidéri, and J.P. Zolésio. Fonctions géométriques principales et paramétrisation de forme adaptée à l’optimisation en aérodynamique. Rapport de Recherche à paraître, INRIA, Septembre 2002.
- [7] G. Farin. *Curves and Surfaces for Computer Aided Geometric Design – A practical Guide*. Computer Science and Scientific Computing. Academic Press, Boston, 2nd edition, 1990.
- [8] S.D. Conte and C. de Boor. *Elementary Numerical Analysis – an algorithmic approach*. McGraw-Hill Book Company, New York, second edition, 1965, 1972.

Contents

1	Introduction	3
2	A series of numerical experiments to evaluate and adapt the parameterization	5
2.1	Bézier curvefit of a function given analytically	5
2.2	Bézier curvefit of the RAE2822 airfoil	6
2.3	Inverse aerodynamic design	6
2.4	Non-unicity of best Bézier curvefit	9
2.5	Bézier curvefit with a regularity constraint based on the total variation	9
2.6	Bézier curvefit with a regularity constraint based on the total length	10
2.7	Drag reduction based on a uniformly-distributed control points	11
2.8	Drag reduction using a parameterization regularized by means of the total variation	12
2.9	Drag reduction using a parameterization regularized by means of the total length .	12
2.10	Drag reduction using a parameterization regularized by optimization of the whole set $\{(x_k, y_k)\}$	12
2.11	Self-adaptive optimization using a weighting function	12
3	Conclusions	17



Unité de recherche INRIA Sophia Antipolis

2004, route des Lucioles - BP 93 - 06902 Sophia Antipolis Cedex (France)

Unité de recherche INRIA Lorraine : LORIA, Technopôle de Nancy-Brabois - Campus scientifique
615, rue du Jardin Botanique - BP 101 - 54602 Villers-lès-Nancy Cedex (France)

Unité de recherche INRIA Rennes : IRISA, Campus universitaire de Beaulieu - 35042 Rennes Cedex (France)

Unité de recherche INRIA Rhône-Alpes : 655, avenue de l'Europe - 38330 Montbonnot-St-Martin (France)

Unité de recherche INRIA Rocquencourt : Domaine de Voluceau - Rocquencourt - BP 105 - 78153 Le Chesnay Cedex (France)

Éditeur

INRIA - Domaine de Voluceau - Rocquencourt, BP 105 - 78153 Le Chesnay Cedex (France)

<http://www.inria.fr>

ISSN 0249-6399